Int J Clin Exp Pathol 2014;7(11):7323-7341
www.ijcep.com /ISSN:1936-2625/IJCEP0002456

Original Article

Effect of chronic usage of tramadol on motor cerebral cortex and testicular tissues of adult male albino rats and the effect of its withdrawal: histological, immunohistochemical and biochemical study

Fatma M Ghoneim[1], Hanaa A Khalaf[1], Ayman Z Elsamanoudy[2], Ahmed N Helaly[3]

[1]Department of Histology and Cell Biology, [2]Department of Medical Biochemistry and Molecular Biology, [3]Department of Forensic Medicine and Toxicology, Faculty of Medicine, Mansoura University, Egypt

Received September 11, 2014; Accepted October 31, 2014; Epub October 15, 2014; Published November 1, 2014

Abstract: This study was designed to demonstrate the histopathological and biochemical changes in rat cerebral cortex and testicles due to chronic usage of tramadol and the effect of withdrawal. Thirty adult male rats weighing 180-200 gm were classified into three groups; group I (control group) group II (10 rats received 50 mg/kg/day of tramadol intraperitoneally for 4 weeks) and group III (10 rats received the same dose as group II then kept 4 weeks later to study the effect of withdrawal). Histological and immunohistochemical examination of cerebral cortex and testicular specimens for Bax (apoptotic marker) were carried out. Testicular specimens were examined by electron microscopy. RT-PCR after RNA extraction from both specimens was done for the genes of some antioxidant enzymes .Also, malondialdehyde (MDA) was measured colourimetrically in tissues homogenizate. The results of this study demonstrated histological changes in testicular and brain tissues in group II compared to group I with increased apoptotic index proved by increased Bax expression. Moreover in this group increased MDA level with decreased gene expression of the antioxidant enzymes revealed oxidative stress. Group III showed signs of improvement but not returned completely normal. It could be concluded that administration of tramadol have histological abnormalities on both cerebral cortex and testicular tissues associated with oxidative stress in these organs. Also, there is increased apoptosis in both organs which regresses with withdrawal. These findings may provide a possible explanation for delayed fertility and psychological changes associated with tramadol abuse.

Keywords: Tramadol, testis, brain, Bax, apoptosis, oxidative stress

Introduction

Tramadol analgesic was manufactured in Germany more than 35 years ago. It is centrally acting analgesic with weak opioid action. It also possesses catecholamine and serotonin reuptake property [1]. Opioids have been used in pain treatment for more than 100 years however prolonged use of opioids may induce addiction resulting in physical and psycho logical dependence. The chronic effect of such drug on cerebral neurons suggests that long term use of opioids may induce the structural alteration of neurons [2]. In a prospective, uncontrolled, non-randomized study, a group of men with an average pain duration of 11 years used intrathecal morphine for 12 weeks. Most of the patients reported poor libido and erectile difficulty toward the end of the 12-week period; in addition, testosterone and follicle stimulating hormone (FSH) levels significantly reduced [3].

Oxidative stress is defined as an imbalance between reactive oxygen species (ROS) production of and the ability to neutralize them *via* antioxidant enzymatic and/or non-enzymatic activity. Large amounts of reactive intermediates lead to cell component damage and production of secondary toxic compounds e.g., reactive aldehydes and ketones [4]. Oxidative stress-related genes are differentially expressed following chronic morphine administration in a rat model in a study done by [5] and they concluded in their study that chronic opioid

administration may be involved in oxidative stress which differs according to the age. Apoptosis or programmed cell death is an active process of normal cell death during development and also, occurs as a result of the cytotoxic effect of various neurotoxins. Previous in vitro studies, indicated that exposure to opioid receptor agonists increases their liability to death by apoptotic mechanisms [6]. In addition, other studies have been revealed that chronic morphine administration in rats is associated with significant changes in the principle proteins involved in the apoptosis signaling which collectively leads to induction of apoptosis [7].

Some studies have linked use of tramadol and its effect biochemically and histopathologically on the brain & testes, but there is very few evidence for withdrawal link of tramadol on these organs. This study was performed to demonstrate the histopathological and biochemical changes in rat cerebral cortex and testicles due to chronic usage of tramadol as well as a 4-weeks spontaneous recovery period to evaluate the reversibility of the toxic effects of long-term administration of tramadol on the cerebral cortex and testicles.

Materials and methods

Drugs

Tramal (Tramadol HCl), 50 mg capsules, was obtained from Mina-Pharm, Egypt. Tramadol hydrochloride is an odourless, white to off-white crystalline powder that is readily soluble in both water and ethanol.

Experimental protocol

The experimental protocol of the study was approved by the ethical committee of Medical Faculty of Mansoura University. Animals were used in accordance with the Animal Welfare Act and Guide for Care Use of MERC (Mansoura Experimental Research Center) prepared by Mansoura University. In this study 30 adult male rats weighing 180-200 gm each were housed in a quite non-stressful environment for one week before study. They were fed ad libitum and allowed free access to water during the experimental period. Animals were divided into three equal groups (10 rats each): Group I: Each animal received 1 ml normal saline 0.9% orally by gavage for 4 weeks and used as control. Group II: Each animal received 50 mg/kg/day (1/5 th LD50) of tramadol intraperitoneally for 4 weeks [8]. Group III: Each animal received the same dose as group II then kept 4 weeks later to study the effect of withdrawal.

At the end of each experiment, all animals were sacrificed and then intracardiac perfusion was done by 2.5% glutraldehyde with 0.1 M phosphate buffer at PH 7.4 for partial fixation of specimens. Testes were removed and craniotomy was performed to dissect out the intact brains for histological, immunohistochemical and electron microscopic studies.

Histological study

Specimens from testis and brain were fixed in Bouin's solution. After fixation, specimens were dehydrated in an ascending series of alcohol, cleared in two changes of xylene and embedded in molten paraffin. Sections of 5 microns thickness were cut using rotary microtome and mounted on clean slides. For histological examination, sections were stained with hematoxylin and eosin (H&E) according to [9].

Immunohistochemical (IHC) study

Sections were taken on positive slides and immunostained using avidin-biotin technique [10]. Slides were deparaffinized, rehydrated, rinsed in tap water, embedded in 0.01% H_2O_2 to block endogenous peroxidase activity and unmasking of the antigenic site was carried out by transmitting sections into 0.01 M citrate buffer (ph 6) for 10 minutes in ethanol for 10 minutes. Then boiling in microwave for 4 minutes at temperature grade VIII followed by 2 minutes at grade II. Incubation in 1/100 normal rabbit serum for 20 minutes was done in order to omit non specific background. The slides were incubated for two hours with the diluted primary antibody at dilution 1/500 & 1/400 biotinylated polyclonal rabbit antibody for BAX. ABC reagent was prepared and left for 30 minutes. Sections were incubated with the avidin-biotin complex (ABC) reagent for 60 minutes then incubated in peroxidase substrate solution for 6-10 minutes. Finally, haematoxylin was used as a counter stain, dehydration in absolute alcohol, clearing and mounting were done. For the negative control slide, the specific 1ry antibody was replaced by phosphate buffer saline. Mice thymus was used as a positive control.

Table 1. Genes' specific primers used for semiquantitative RT-PCR

Gene	Primer	Gene bank accession no	Reference
Glutathione peroxidase	Forward 5'-ATG CCC CGC TCT ACT TCC-3' Reverse 5'-GAA CAC CGT CTG GAC CTA CC-3'	X07365	[15]
Cu/Zn-SOD	Forward 5'-AAC TGA AGG CGA GCA TGG-3' Reverse 5'-ATC ACA CCA CAA GCC AAGC-3'	M21060	[15]
Mn-SOD	Forward 5'-CAC CAC AGC AAG CAC CAC-3' Reverse 5'-TCC CAC ACA TCA ATC CCC-3'	Y00497	[15]
Catalase	Forward 5'-GCT CCC AAC TAC TAC CCC AAC-3' Reverse 5'-CGT TTC CTC TCC TCC TCA TTC-3'	M11670	[15]
Internal house keeping (control) gene (GAPDH)	Forward 5'-GGCTGCCTTCTCTTGTGAC-3' Reverse 5'-GGCCGCCTGCTTCACCA-3'	AF106860	[16]

Table 2. Thermal Cycling programs for semiquantitative RT-PCR of genes studied

	Glutathione peroxidase	Cu/Zn-SOD	Mn-SOD	Catalase	GAPDH (internal control, House keeping gene)
Initial denaturation	95°C for 10 minutes	95°C for 10 minutes	95°C for 10 minutes	95°C for 10 minutes	94°C for 5 minutes
Cycles					
Number	27	27	26	27	25
Denaturation	94°C for 1 minute	94°C for 30 seconds	94°C for 1 minute	94°C for 1 minute	95°C for 30 seconds
primer annealing	59°C for 1 minute	56°C for 30 seconds	62°C for 1 minute	62°C for 1 minute	62.5°C for 30 seconds
Extension	72°C for 1 minute	72°C for 1 minute	72°C for 1 minute	72°C for 1 minute	72°C for 2 minute
Final extension	72°C for 10 minutes	72°C for 10 minutes	72°C for 10 minutes	72°C for 10 minutes	72°C for 7 minutes
Product size	301 bp	333 bp	410 bp	173 bp	721 bp

Commercial monoclonal antibodies (Polyclonal rabbit antimouse/rat Bax antibody, Pharmingen, Becton Dickinson Company, San Diego, CA 92121, USA) and DAKO EnVisionTM + System, HRP/DAB (rabbit ready-to-use detection system using the labeled polymer method, DAKO Corporation, Carpimena, CA 93013, USA).This kit is used to stain membrane, cytoplasmic and nuclear antigens.

Semi-quantification analysis of the apoptotic index (AI) was determined by counting a total of at least 1000 cells per slide subdivided in 10 fields chosen randomly at × 400 magnification. AI% = [number of positive cells/total number of calculated cells] × 100 is the percentage of positive cells in 1000 cells [11].

Electron microscopic study

For transmission electron microscopy, small pieces of testis were fixed in 2.5% glutaraldehyde buffered with 0.1 M cacodylate (pH 7.2) for 2 hours. The specimens were washed three times with the same buffer and post fixed in phosphate-buffered 1% osmium tetroxide for 2 hours at room temperature then dehydrated in ascending grades of ethanol. After immersion in propylene oxide, specimens were embedded in epoxy resin mixture. Semithin sections (1 um thick) were obtained and stained with 1% toluidine blue and examined by light microscope. Ultrathin sections (80-90 nm) were cut by LKB ultratome and stained with uranyl acetate and lead citrate [12]. The ultrastructural analysis was carried out with transmission electron microscope (Joel TEM CS 100) in the Electron Microscopic Unit, Faculty of Science El-Shatby, Alexandria University.

Semiquantitative reverse transciptase-PCR

Total RNA was extracted from Brain and testicular tissue, the tissue sample of each was

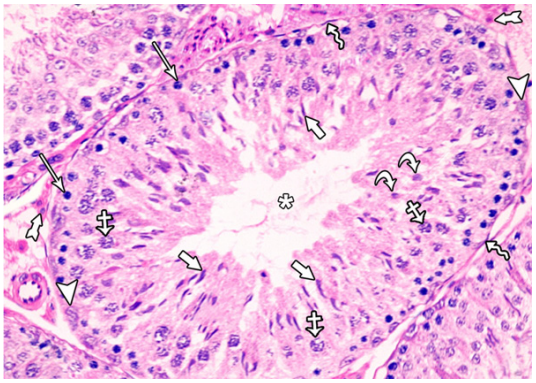

Figure 1. A photomicrograph of a section from the testis of a rat of the control group showing seminiferous tubules and interstitial tissue. Each tubule was lined with stratified epithelium (spermatogenic cells) and supporting Sertoli cells. The healthy spermatogenic cells include spermatogonia (arrows), primary spermatocytes (crossed arrows), round (early) spermatid (curved arrows), elongated (late) spermatid (short arrows) and spermatozoa (asterisk). Notice the presence of: Myoid cells (zigzag arrow), Sertoli cells (arrow heads) and interstitial cells leydig (tailed arrow).

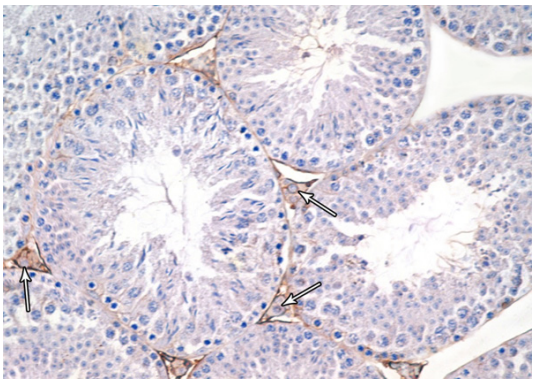

Figure 2. A photomicrograph of a section from the testis of a rat from the group I showing mild Bax-positive reaction in leydig cells (Bax immunostaining × 400).

shock freezed by liquid nitrogen and used immediately for RNA extraction using TriFast™ reagent (PeqLab. Biotechnologie GmbH, Carl-Thiersch St. 2B 91052 Erlongen, Germany, Cat. No. 30-2010) according to the manufacturer's instructions. The remaining DNA was removed by digestion with DNase I (Sigma). The concentration of isolated RNA was determined spectrophotometrically by measuring the optical density (OD) at 260 nm (Jenway, Genova Model, UK). 10 µl of each sample was added to 990 µl of DEPC treated water and quantified by measuring the absorbance at 260 nm as RNA yield (µg/ml) = A260 × 40 × 100 (dilution factor) [13]. The purity of RNA was determined by gel electrophoresis through formaldehyde agarose gel electrophoresis and ethidium bromide staining to show 2 sharp purified bands, these two bands represented 28S and 18S ribosomal RNA.

RT-PCR was performed using Ready-to-Go RT-PCR beads for first cDNA synthesis and PCR reaction provided by Amersham Biosciences, England. Cat. No. 27-9266-01, according to the method of [14]. Ready-to-Go RT-PCR beads utilize Moloney Murine leukemia virus (*M-MuLV)* reverse transcriptase and Taq polymerase to generate PCR product from RNA template. Each bead is optimized to allow the first strand cDNA synthesis and PCR reaction to proceed sequentially as a single tube, single step reaction. The reaction passed as follow:

Synthesis of cDNA: The followings were added to each tube containing the beads: 2 µl of first strand primer, provided by the kit, 3 µl containing 30 pmol of PCR gene-specific primer (sense), 3 µl containing 30 pmol of PCR gene-specific primer (anti-sense), 25 µl of total template RNA containing 1ug and 17 µl of DEPC-treated water to obtain a total volume of 50 µl. One tube was prepared as a negative control reaction to test for DNA contamination. The dehydrated bead (without template and primers) was incubated at 95°C for 10 minutes to inactivate the M-MuLV reverse transcriptase. 50 ul mineral oil were added to overlay the reaction. The reactions were transferred to the thermal cycler and incubated at 40°C for 30 minutes for synthesis of cDNA followed by incubation at 95°C for 5 minutes to inactivate the reverse transcriptase and completely denature the template.

Gene specific primers were purchased from Biolegio. BV, PO Box 91, 5600 AB Nijmegen, Netherlands. Primers sequences are presented in **Table 1**.

Amplification of cDNA by PCR: Thermal cycling reaction was performed using thermal cycler (TECHEN TC-312, Model FTC3102D, Barloworld Scientific Ltd. Stone, Stafford Shire st., 150 SA, UK) with the following program (**Table 2**).

Detection of amplified RT-PCR products: For semiquantitative RT-PCR, the products of amplification were subjected to agarose gel

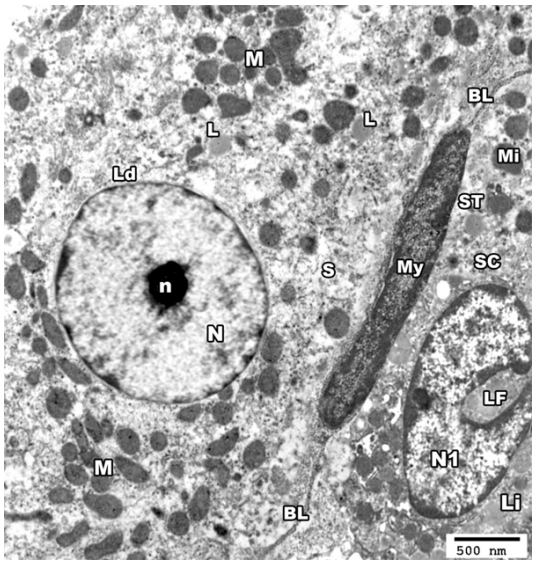

Figure 3. An electron micrograph of a section from the testis of a rat from group I showing the basal lamina (BL) of seminiferous tubule (ST) and a myoid cell (My). The nucleus (N1) of sertoli cell (SC) shows a characteristic longitudinal fold (LF) and a rim of peripheral dense chromatin, the cytoplasm contains mitochondria (Mi) and lipid droplets (Li). The interstitial tissue revealed Leydig cell (Ld) having large rounded euchromatic nucleus (N) with a prominent nucleolus (n), its cytoplasm contains mitochondria (M), SER (S) and some lipid droplets (L) (TEM × 3000).

electrophoresis using 2% agarose stained with ethidium bromide and visualized via light UV Transilluminator (Model TUV-20, OWI Scientific, Inc. 800 242-5560, France) and photographed under fixed conditions (the distance, the light and the zoom) (**Figure 29**).

The results photos were analyzed with scion image ® release Alpha 4.0.3.2. Software for windows ® which performs bands detection and conversion to peaks. Area under each peak were calculated in square pixels and used for quantification. Gene expression levels were determined by calculating the ratio between the square pixel values of the target gene in relation to the internal house keeping control gene (GAPDH).

Negative control tubes showed no PCR products indicating that all reagents were free from target sequence contamination.

Tissue homogenate preparation

Brain and testicular tissues were perfused with a PBS (phosphate buffered saline) solution, pH 7.4 containing 0.16 mg/ml heparin to remove any red blood cells and clots. Then, each tissue sample was homogenized in 5-10 ml cold buffer (i.e. 50 mM potassium phosphate, pH 7.5. 1 mM EDTA). Homogenates were centrifuged at 10000 × *g* for 15 minutes at 4°C and the supernatant was kept at -80°C till used for analysis of lipid peroxides (malondialdehyde, MDA) which were analyzed by the method of [17] using colorimetric kit (Bio-Diagnostics, Dokki, Giza, Egypt, Cat. No. # MD 2528). The value is expressed as nmol/g tissue.

Statistical analysis

Data are expressed as mean value ± SD. Comparisons were carried out by analysis of variance followed by Tukey's test, using SPSS for Windows (15.0 Version). Differences were considered statistically significant when $P < 0.05$. Pearson correlation was used to assess relations between variables [18].

Results

Pathological changes of the testis

Group I

Light microscopy: Histological examination of testis of control rat stained with H&E showed normal appearance of seminiferous tubules and interstitial tissue. Each tubule was lined with stratified epithelium (germinal cells) and supporting Sertoli cells. The germinal cells were arranged in the form of many layers from the basement membrane toward the lumen of the tubules. These layers are formed of spermatogenic cells, which are; spermatogonia, primary spermatocytes, spermatids and mature sperms. The connective tissue stroma between the tubules contained interstitial cells of Leydig (**Figure 1**). In immunohistochemicaly stained sections, Leydig cells showed mild immunestain reaction for Bax (**Figure 2**).

Electron microscopy: Electron microscopic examination of the control group showed the basal lamina surrounded the seminiferous tubule and included a myoid cell. Sertoli cell showed the nucleus with its characteristic longitudinal fold and a rim of peripheral dense chromatin. The cytoplasm contained mitochondria and lipid droplets. The interstitial tissue revealed Leydig cell having large euchromatic nucleus with a prominent nucleolus and a rim of peripheral dense chromatin. The cytoplasm

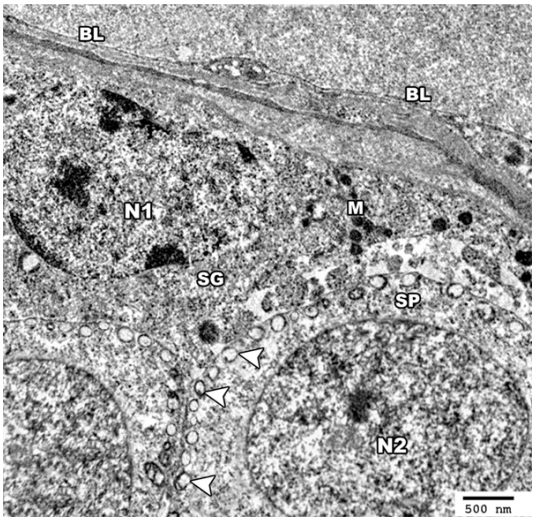

Figure 4. An electron micrograph of a section from the testis of a rat of group I showing the germinal cells based on the basal lamina (BL) of seminiferous tubule. The spermatogonial cell (SG) shows a pale stained nucleus (N1) with peripheral chromatin clumps and the cytoplasm contains mitochondria (M). The primary spermatocyte (SP) shows a rounded euchromatic nucleus (N2) and peripherally arranged mitochondria in the cytoplasm (arrow head) (TEM × 3000).

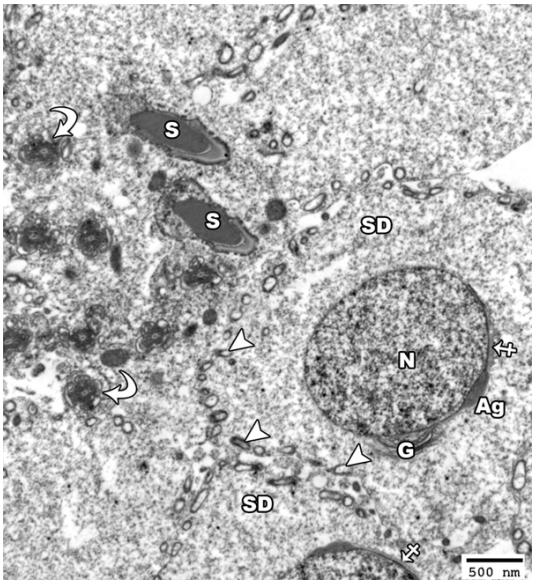

Figure 5. An electron micrograph of a section from the testis of a rat from the group I showing a spermatid (SD) with a rounded euchromatic nucleus (N) covered on the proximal part of its circumference with acrosomal vesicle (crossed arrow) and acrosomal granule (Ag). The cytoplasm shows peripherally-arranged mitochondria with clear matrix (arrow head) as well as a well-developed golgi apparatus at one side of the nucleus (G). Note the presence of the head of mature sperm had a pyramidal dark nucleus covered by acrosomal cap (S) and the transverse section in the middle piece (curved arrow) showed centrally located microtubules which form the axoneme of the mature sperm (TEM × 2500).

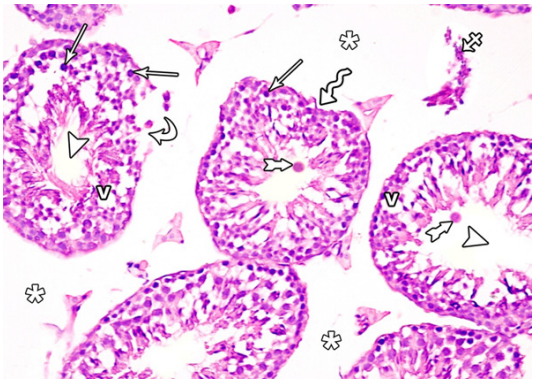

Figure 6. A photomicrograph of a section from the testis of a rat of group II showing irregular seminiferous tubules (zigzag arrow) and ruptured one (curved arrows). The seminiferous tubules show absence of spermatozoa (arrow head). Many vacuoles among the spermatogenic cells (V), pyknotic nuclei (arrow) and multinucleated giant cells (tailed arrow) are evident. Note, widening of the interstitial space (asterisks) and inflammatory cells in it (crossed arrow) (H&E × 400).

contained mitochondria, smooth endoplasmic reticulum (SER) and some lipid droplets (**Figure 3**).

Spermatogonial cell appeared with pale stained nucleus which showed peripheral chromatin clumps and the cytoplasm contained mitochondria. The primary spermatocyte had a rounded nucleus and peripherally arranged mitochondria in the cytoplasm (**Figure 4**). The spermatids had a rounded nucleus and many peripherally-arranged mitochondria with clear matrix as well as a well-developed Golgi apparatus at one side of the nucleus. Furthermore, it could be noticed that the acrosomal granule appeared as an ovoid deep condensation enclosed in the acrosomal vesicle covering one third of the nucleus to form the acrosome. The head of mature sperm had a pyramidal dark nucleus covered by acrosomal cap. Transverse section in the middle piece showed centrally located microtubules which form the axoneme of the flagellum (**Figure 5**).

Group II

Light microscopy: Animals received tramadol for 4 weeks showed distinct histological chang-

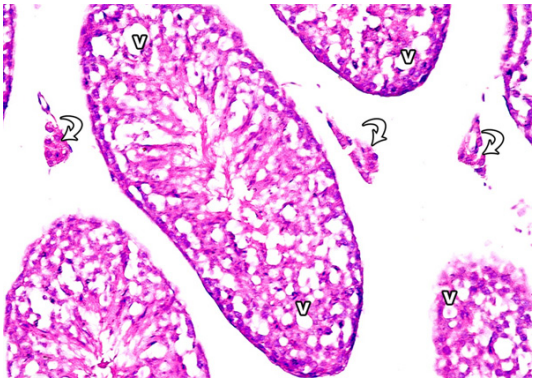

Figure 7. A photomicrograph of a section from the testis of a rat from group II showing many vacuoles (v) in between the degenerated germ cells and reduced leydig cell concentration (curved arrows) (H&E × 400) compared to **Figure 1**.

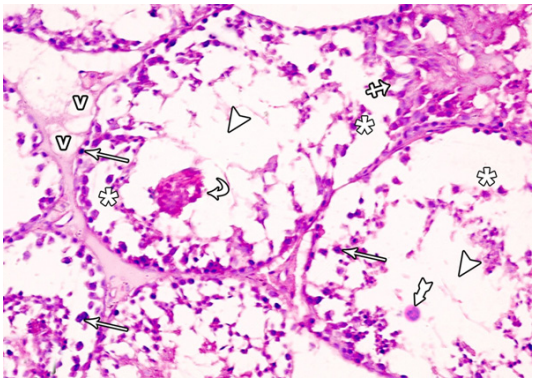

Figure 8. A photomicrograph of a section from the testis of a rat from group II showing ruptured seminiferous tubule (crossed arrow) with damaged and disorganized spermatogenic cells which are lifting off the basal lamina (asterisks) and some of them are exfoliated in the lumen of the tubule (curved arrows). Note the pyknotic nuclei (arrows), vacuoles (v) in the interstitial space, absence of spermatozoa (arrow heads) and multinucleated giant cells (tailed arrow) (H&E × 400).

es. The seminiferous tubules appeared with irregular outline, widely separated from each other and rupture of some tubules was observed with absence of spermatozoa. Many vacuoles among the spermatogenic cells, apoptotic cells and multinucleated giant cells were found. The intertubular tissue showed many inflammatory cells (**Figure 6**). Leydig cells were reduced in number and many vacuoles in between the degenerated germ cells were seen (**Figure 7**). The majority of the seminiferous tubules exhibited damaged and disorganized spermatogenesis cells and the damaged germ

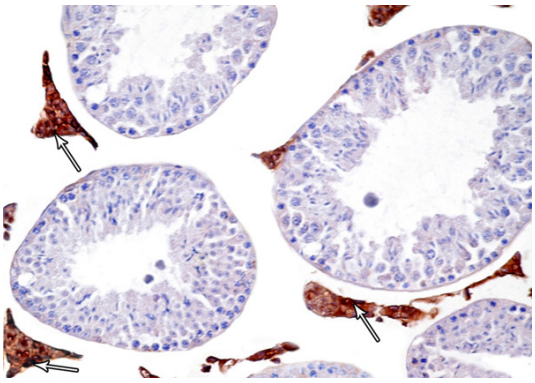

Figure 9. A photomicrograph of a section from the testis of a rat of group II showing intense Bax-positive reaction in leydig cells (arrows). (Bax immunostaining × 400).

cells were lifting off the basal lamina and some of them were exfoliated in the lumen. Moreover, absence of spermatozoa was clearly recognized. Many spematocytes appeared with pyknotic nuclei and also numerous vacuoles of variable sizes were seen in both the seminiferous tubules and interstitial connective tissue. Some seminiferous tubules appeared ruptured (**Figure 8**). Immunostain for Bax showed intense + ve reaction in Leydig cells (**Figure 9**).

Electron microscopy: In transmission electron microscope of tramadol treated group, the seminiferous tubules appeared with a wavy thickened basement membrane and the interstitial tissue showed mononuclear cell infiltration (eosinophil) and congested capillaries. The nuclei of leydig cells became irregular in shape and some nuclei were shrunken and hyperchromatic. Their cytoplasm showed dilated smooth endoplasmic reticulum and many vacuoles (**Figure 10**).

The nuclei of spermatogonia were hyperchromatic and showed irregular clumps of heterochromatin and perinuclear haloes. The cytoplasm contained many disrupted mitochondria and numerous vacuoles were seen in between the cells (**Figure 11**). The primary spermatocytes appeared with disrupted and less peripheral mitochondria and its nucleus showed clumps of a peripheral dense chromatin. Mature sperms were found abnormally near to the primary spermatocytes (**Figure 12**). Some spermatocytes appeared with irregular clumps of heterochromatin in the nucleus and with disrupted mitochondria and vacuoles in the cytoplasm (**Figure 13**).

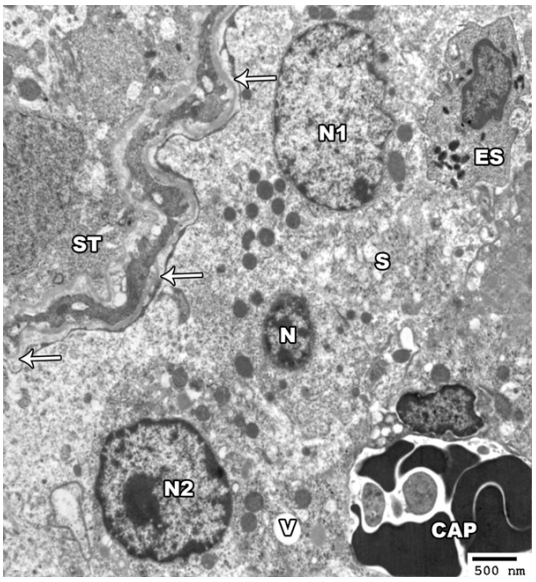

Figure 10. An electron micrograph of a section from the testis of a rat of group II showing the seminiferous tubules (ST) with a wavy, thickened basement membrane (arrow). The interstitial tissue contains eosinophil (ES) and congested capillaries (CAP). The leydig cells show irregular nuclei (N1-N2) and shrunken hyperchromatic one (N). Their cytoplasm show dilated smooth endoplasmic reticulum (S) and vacuoles (V) (TEM × 2000).

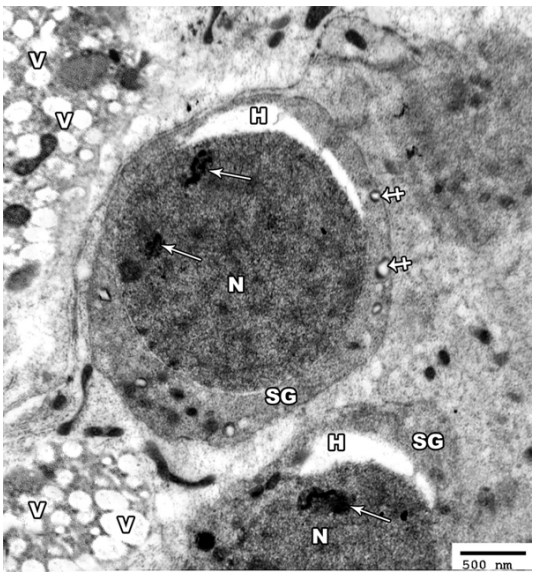

Figure 11. An electron micrograph of a section from the testis of a rat of group II showing hyperchromatic nucleus (N) of the spermatogonic cells (SG) with irregular clumps of heterochromatin (arrow). The cytoplasm contains many distorted mitochondria (crossed arrow). Note the presence of perinuclear haloes (H) and many vacuoles (V) in between the cells (TEM × 3000).

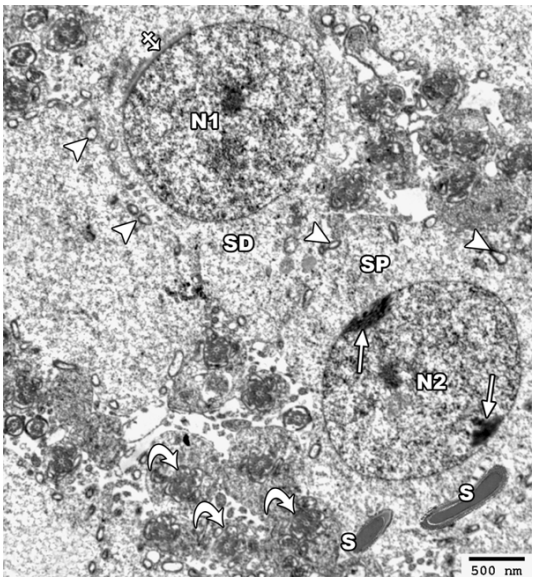

Figure 12. An electron micrograph of a section from the testis of a rat of group II showing a primary spermatocyte (SP) with its nucleus (N2) showing clumps of a peripheral heterochromatin (arrow). Mature sperms with its head (S) and axoneme (curved arrow) are present abnormally near the primary spermatocyte. The spermatide cell (SD) appears with its rounded nucleus (N1) that is covered on the proximal part of its circumference with the acrosomal cap (crossed arrow). Note the presence of few disrupted mitochondria (arrow head) (TEM × 2500).

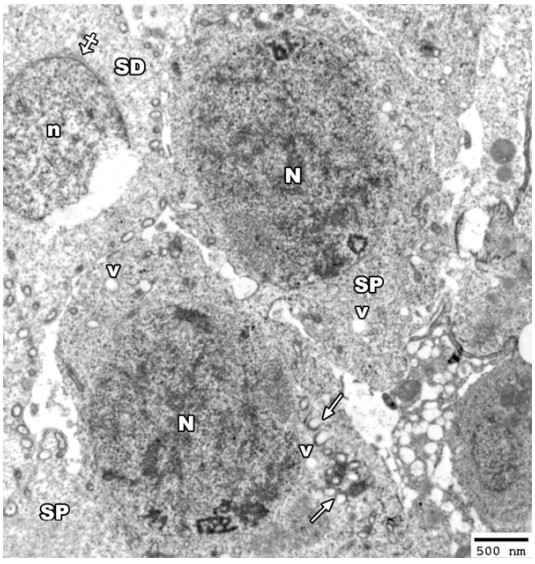

Figure 13. An electron micrograph of a section from the testis of a rat from group II showing two primary spermatocytes (SP) with heterochromatic nucleus (N) and the cytoplasm contains disrupted mitochondria (arrow) and many vacuoles (V). Note, the rupture of the nucleus (n) of early spermatid (SD) with appearance acrosomal cap (crossed arrow) (TEM × 2500).

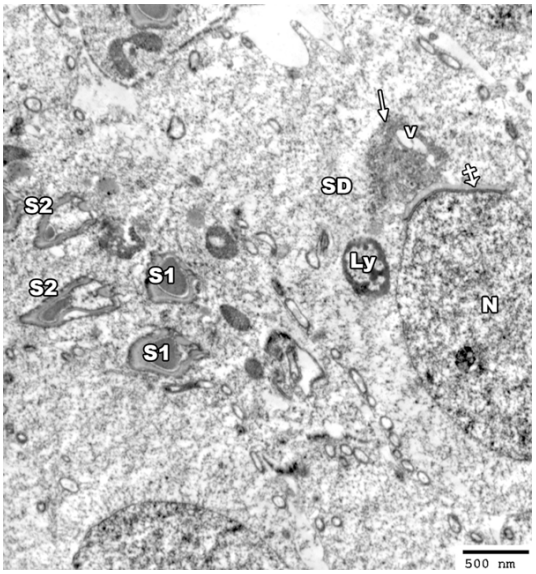

Figure 14. An electron micrograph of a section from the testis of a rat from group II showing spermatid cell (SD) with elongated nucleus (N) covered by acrosomal cap (crossed arrow) and vacuolated (V) golgi apparatus (arrow). The cytoplasm contains lysosomes (LY). The head of some sperms shows abnormally shaped nucleus (S1) and other sperms show degenerated heads (S2) (TEM × 3000).

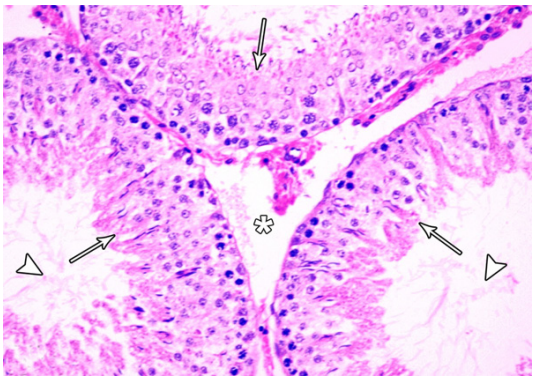

Figure 15. A photomicrograph of a section from the testis of a rat from group III showing increased spermatogenic cell layers (arrow), increased sperm bundles (arrow head) and normal spaces between the tubules (asterisks) (H&E × 400).

The electron micrograph of the early spermatid showed that the nuclei of some of them exhibited degenerative changes in the form of ruptured nuclear membrane (**Figure 13**). Lysosomes and golgi apparatus with vacuoles were detected in the cytoplasm. The head of some sperms showed abnormally shaped nucleus and other sperms showed degenerated heads (**Figure 14**).

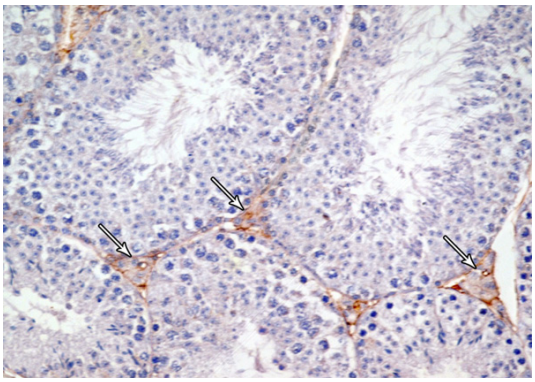

Figure 16. A photomicrograph of a section from the testis of a rat from group III showing mild Bax-positive reaction in leydig cells (arrow) (Bax immunostaining × 400).

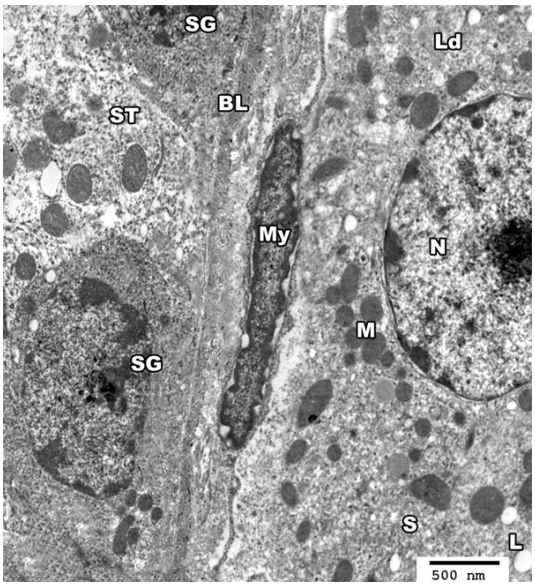

Figure 17. An electron micrograph of a section from the testis of a rat of group III showing basal lamina (BL) of seminiferous tubule (ST), a myoid cell (MY) as well as spermatogonic cells (SG). The interstitial cell of leydig (Ld) appears with euchromatic nucleus (N). The cytoplasm contains mitochondria (M), smooth endoplasmic reticulum (S) and lipid droplets (L) (TEM × 3000).

Group III

Light microscopy: Examination of testis sections of this group revealed less prominent histopathological changes when compared with tramadol group. Most of the seminiferous tubules appeared with increased spermatogenic cell layers and with increase in the number of sperm bundles. The spaces between the seminiferous tubules were reduced in size (**Figure**

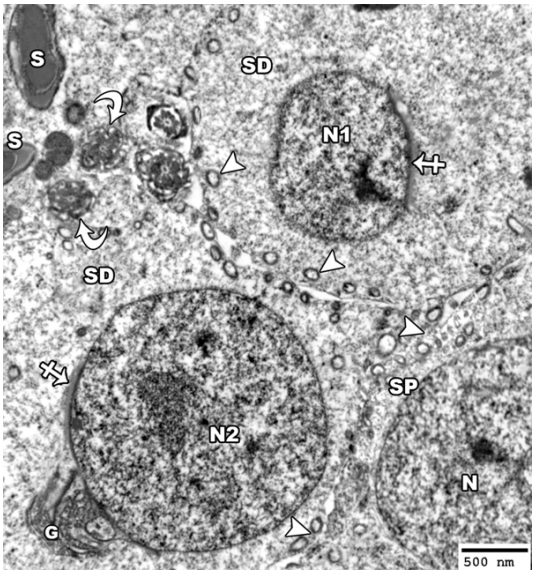

Figure 18. An electron micrograph of a section from the testis of a rat of group III showing a spermatid cell with shrunken nucleus (N1) and another cell with normal nucleus (N2). The nuclei of both cells are covered by acrosomal cap (crossed arrow) and the cytoplasm shows golgi saccules (G) and mitochondria (arrow head). The mature sperm with its head (S) and axoneme (curved arrow) appears nearly normal in structure and position to that of group I. Note the presence of primary spermatocyte (SP) with euchromatic nucleus (N) and peripheral mitochondria (arrow head) (TEM × 3000).

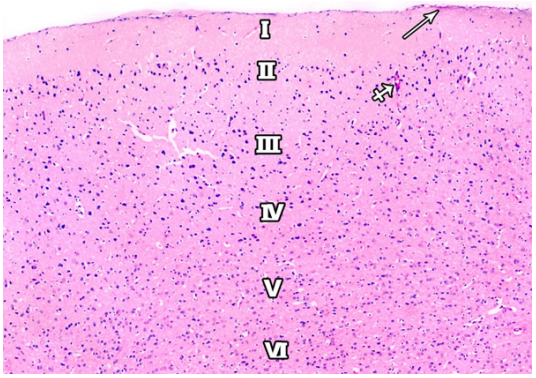

Figure 19. A photomicrograph of a section of the frontal motor area of cerebral cortex of a rat from group I showing a delicate layer of pia matter (arrow) and six layers of the motor cortex are demonstrated; outer molecular (I); external granular (II), external pyramidal (III); inner granular (IV); inner pyramidal (V); and the polymorphic layer (VI). Blood capillaries (crossed arrows) are also observed (H&E × 100).

15). Immunostain for Bax showed mild reaction nearly as control (**Figure 16**).

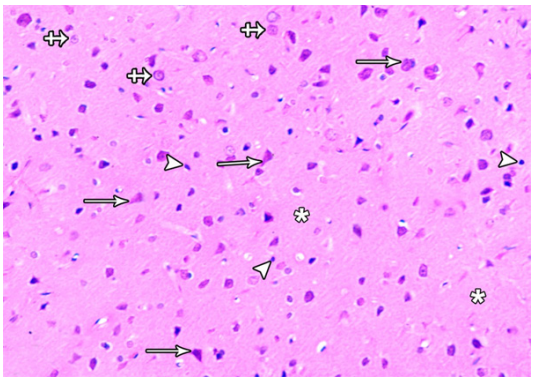

Figure 20. A Photomicrograph showing the inner pyramidal layer of the frontal motor cortex in the control group. Large pyramidal cells (arrows) with basophilic cytoplasm, large vesicular nucleus and long apical dendrite are observed. Granular cells (crossed arrows) with large rounded vesicular nuclei are detected. The glial cells (arrow heads) with small dense nuclei are also seen. Note, eosinophilic neuropil (asterisks) forming the background for the cells (H&E × 400).

Electron microscopy: Electron microscopic examination of group III showed the seminiferous tubules with intact basal lamina enclosing the myoid cell. The interstitial cells of leydig had euchromatic nucleus with peripheral clumps of heterochromatin. Their cytoplasm showed mitochondria, smooth endoplasmic reticulum and lipid droplets (**Figure 17**).

As regard spermatids, some appeared with normal nucleus but others appeared with shrunken nucleus. Their cytoplasm contained mitochondria and golgi apparatus. The mature sperm was normal in position and its head appeared with a pyramidal dark elongated nucleus covered by acrosomal cap and the cytoplasm showed many mitochondria. The primary spermatocyte appeared with euchromatic nucleus and with increased number of the peripheral mitochondria (**Figure 18**).

Pathological changes of the cerebrum

Group I

Examination of H&E stained sections of control group showed that the cerebral cortex showed groups of nerve cells arranged in well organized six layers, outer molecular layer covered with pia mater, outer granular layer, outer pyramidal layer, inner granular layer, inner pyramidal and polymorphic layers (**Figure 19**). The pyramidal cells showed open face nuclei, basophilic cyto-

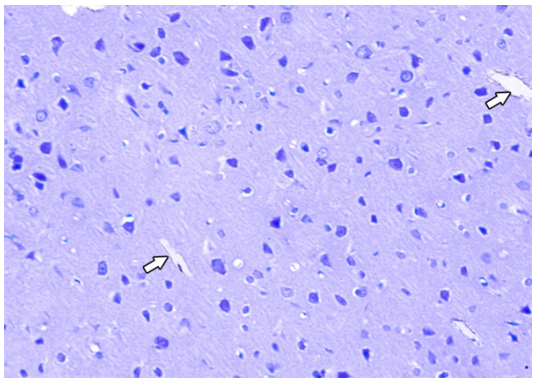

Figure 21. A photomicrograph showing Bax-negative immunoreaction in the cells of the frontal motor area of the cerebral cortex in the control group. Notice the presence of the blood vessels (thick arrow) (Bax immunostaining × 400).

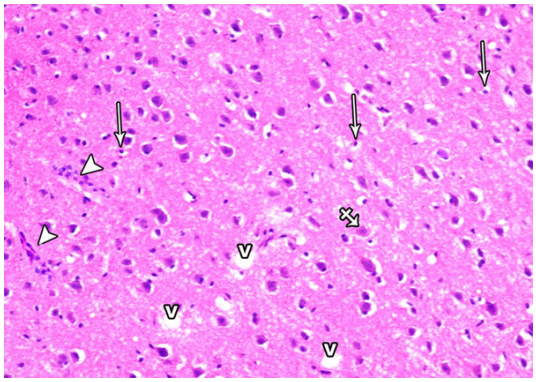

Figure 22. A photomicrograph of a section from the frontal motor area of the cerebral cortex of a rat of group II showing neuronal cell disorganization and hypercellularity as well as increased apoptotic cells (arrow), multinuclear giant cells (crossed arrow) extensive neuropil vacuolization (V) and inflammatory cell infiltrations (arrow head) (H&E × 400).

plasm and long apical dendrite. The granular cells appeared rounded in shape and showed large rounded vesicular nuclei with prominent nucleoli. Glial cells appeared smaller in size with small deeply stained nuclei. The ground substance between the nerve cells is normally occupied with homogenous eosinophilic background (neuropil) formed of neuronal and glial cell processes (**Figure 20**). No Bax-postive cells could be observed in the immunostained sections of the control group (**Figure 21**).

Group II

Examination of Hx&E stained sections of tramadol treated group showed marked disorganization of the cortical layers and hypercellularity

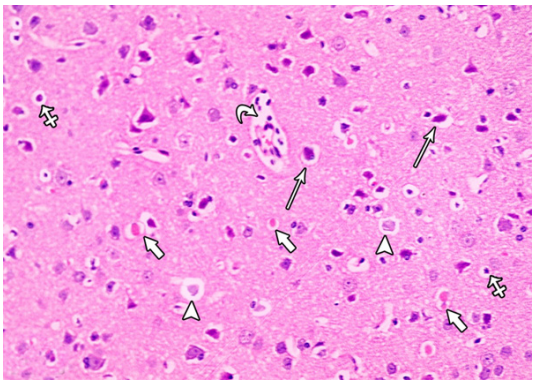

Figure 23. A photomicrograph of a section from the frontal motor area of the cerebral cortex of a rat of group II showing some irregular darkly stained pyramidal cells with pyknotic nuclei and surrounded by haloes (arrows) others are shrunken and shows marked cytoplasmic vacuolization (crossed arrow). Some pyramidal cells appear with faintly stained cytoplasm and nuclei (arrow head). Note the presence of dilated congested blood vessels with inflammatory cells in it (curved arrow) and the red neurons (short arrow) (H&E × 400).

as well as increased apoptotic cells. Additionally, extensive neuropil vacuolization and multinuclear giant cells were also seen (**Figure 22**). Almost all pyramidal cells appeared irregular in shape, darkly stained with pyknotic nuclei and surrounded by haloes others were shrunken and showed marked cytoplasmic vacuolization. Some pyramidal cells appeared with faintly stained cytoplasm and nuclei. Some regions of the neuropil showed dilated blood vessels, cellular infilterate and red neurons (neurons with hypoxic changes) (**Figure 23**). Numerous Bax-positive cells could be observed in the immunostained sections of group II. Moreover, small masses surrounded by haloes and showed positive immunoreaction for Bax were observed in the different layers of the frontal motor area. Many Bax-positive cells were also observed close to the site of blood vessels (**Figure 24**).

Group III

Light microscopic examination of cortical regions of group III showed return of brain tissues towards normal morphology as evidenced by decreased cellularity and decreased perineuronal haloes as well as normal blood vessels. Multiple pyramidal cells and granular cells appeared normal; however, few pyramidal cells are shrunken and surrounded by haloes (**Figure 25**). The distribution of the positively stained

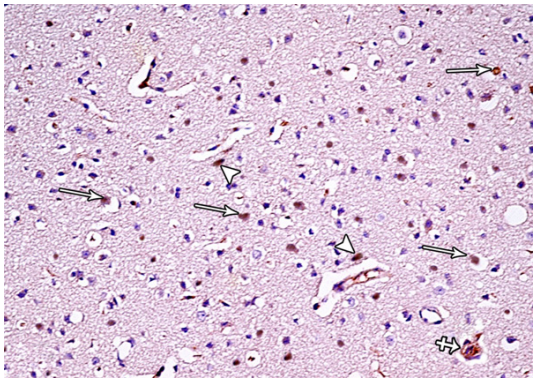

Figure 24. A photomicrograph of a section from the frontal motor area of the cerebral cortex of a rat from group II showing numerous Bax-positive cells (arrows), small masses surrounded by haloes and shows positive immunoreaction for Bax (crossed arrow) and many Bax-positive cells are seen close to the blood vessels (arrow head) (Bax immunostaining × 400).

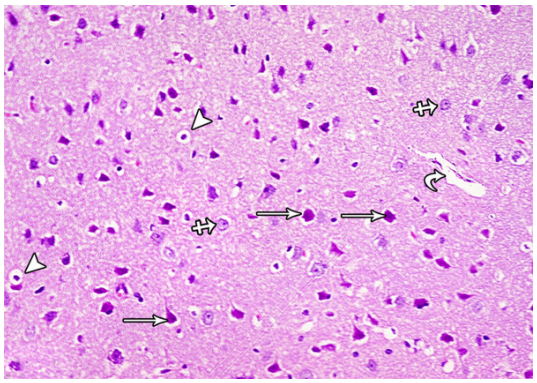

Figure 25. A photomicrograph of a section from the frontal motor area of the cerebral cortex of a rat of group III showing normal pyramidal cells (arrow), granular cells (crossed arrow) and blood vessel (curved arrow). Some pyramidal cells are shrunken and surrounded by haloes (arrow head) (H&E × 400).

neuronal cell by Bax was decreased (**Figure 26**).

Morphometric findings

In **Tables 3**, **4**, the results of the current study showed significant decrease in the gene expression of the antioxidant enzymes (Cu-Zn SOD, Mn-SOD, Catalase and Glutathione peroxidase) in both brain and testicular tissues in group II when compared with the control group while they showed no significant decrease in group III when compared with group I. When comparing group III with group II, there was significant

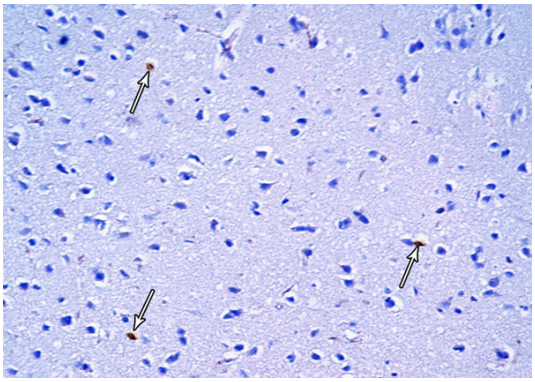

Figure 26. A photomicrograph of a section from the frontal motor area of the cerebral cortex of a rat from group III showing few Bax-positive cells (arrows) (Bax immunostaining × 400).

increase in the gene expression of these enzymes.

Malondialdehyde (MDA) levels of the tissue extract homogenisate of these 2 organs showed statistically significant increase in group II when compared to group I indicating increase in the oxidative stress in such group . While, it shows significant decrease in group III than group II with non significant increase than that of group I.

Apoptotic index (Bax immunohistochemically positive cells) showed significant increase in group II than group I, significant decrease in group III than group II but no significant increase in group III when compared to group I.

(**Figures 27**, **28**) represent the correlation between apoptotic Index and the different studied biochemical parameters in all studied groups and it showed that there were statistically significant positive correlation with MDA levels in both organs (brain and testes) while, it showed statistically significant negative correlation with the gene expression of all of the studied antioxidant enzymes (Cu-Zn SOD, Mn-SOD, Catalase and Glutathione peroxidase).

Discussion

The current study aimed to investigate the possible effects of tramadol administration on rat cerebral cortex and testicles focusing on oxidative stress and apoptosis in these organs. Moreover, to study the light and electron micro-

Table 3. Apoptotic Index (Bax) and antioxidant enzymes gene expression in the different studied groups in the brain

	Groups						ANOVA *P* value	P1	P2	P3
	Group I		Group II		Group III					
	Mean	SD	Mean	SD	Mean	SD				
Cu/Zn-SOD/GAPDH	1.240	0.231	0.716	0.121	1.070	0.246	<0.001	<0.001	0.17	0.002
Mn-SOD/GAPDH	1.957	0.540	1.031	0.355	1.827	0.445	<0.001	<0.001	0.79	0.001
Catalase/GAPDH	0.984	0.282	0.604	0.099	0.933	0.191	0.001	0.001	0.84	0.003
Glutathione peroxidase/GAPDH	2.520	0.508	1.501	0.421	2.199	0.524	<0.001	<0.001	0.31	0.009
MDA	23.103	5.120	132.996	38.304	44.055	11.228	<0.001	<0.001	0.12	<0.001
Bax (apoptotic Index)	1.84	.47	28.320	7.051	6.05	2.01	<0.001	<0.001	0.08	<0.001

SD: standard deviation; P: Probability; P1: Significance of Tramadol group relative to control group; P2: Significance of Withdrawal group relative to control group; P3: Significance of Withdrawal group relative to Tramadol group.

Table 4. Apoptotic Index (Bax) and antioxidant enzymes gene expression in the different studied groups in the testes

	Groups						ANOVA P value	P1	P2	P3
	Group I		Group II		Group III					
	Mean	SD	Mean	SD	Mean	SD				
Cu/Zn-SOD/GAPDH	1.439	0.203	0.909	0.225	1.224	0.218	<0.001	<0.001	0.08	0.008
Mn-SOD/GAPDH	2.103	0.526	1.406	0.274	1.891	0.282	0.001	0.001	0.4	0.02
Catalase/GAPDH	1.099	0.380	0.512	0.102	0.837	0.127	<0.001	<0.001	0.053	0.01
Glutathione peroxidase/GAPDH	3.159	0.441	1.888	0.395	2.789	0.840	<0.001	<0.001	0.35	0.006
MDA	27.964	5.472	123.158	24.756	45.870	12.973	<0.001	<0.001	0.055	<0.001
Bax(apoptotic Index)	6.180	1.471	33.874	10.085	11.623	2.614	<0.001	<0.001	0.13	<0.001

SD: standard deviation; P: Probability; P1: Significance of Tramadol group relative to control group; P2: Significance of Withdrawal group relative to control group; P3: Significance of Withdrawal group relative to Tramadol group.

scopic changes of these two organs in both tramadol treated rats as well as rats under withdrawal.

In the present study, there was statistically significant decrease in the gene expression of the antioxidant enzymes (Glutathione peroxidase, Cu/Zn-SOD, Mn-SOD and catalase) in both brain and testicular tissues with significant increase in MDA (a lipid peroxidation products) in the tissue homogenisate of both tissues in group II (rats with chronic tramadol administration at 50 mg/kg/day) when compared to group I (control group). At the molecular level there was a decrease in the mRNA gene expression of the antioxidanat enzymes associated with an increase in MDA level in the tissue homogenisates in brain and testicular tissues.

These results indicate that tramadol induces oxidative stress in both brain and testicular tissues. This is in agreement with [19-22]. Tramadol belongs to the synthetic opioid analgesic that commonly prescribed for moderate to severe pain at a usual doses being up to 200 mg/day [23]. Tramadol is one of the synthetic opoids that has toxic effects at the cellular level by increasing lipid peroxidation that can be used as a marker of the ROS-induced cell damages [20]. Moreover, it has been found that lipid peroxidation is significantly increased in chronic heroin users [24]. These data are confirmed by the results of previous studies done by [25, 26, 20] as they demonstrated that treatment with morphine and tramadol yielded an increased MDA level, which suggests an increased lipid peroxidation In addition, they observed a decrease in the level of reduced glutathione in the isolated rat hepatocytes in the case of incubation with different opioids concentration (yielding cell death) and they also, noticed a lowered content of reduced glutathione and activities of catalase, superoxide dismutase and glutathione peroxidase .

The oxidative stress induced by tramadol in the brain was reported by [27, 28]. They explained this by those complexes I, III, and IV of electron transfer chain (ETC) in mitochondria were found to be inhibited by tramadol at high doses. Inhibition of complex III resulted in the generation of reactive oxygen species as a consequence of the intrinsic characteristics of the

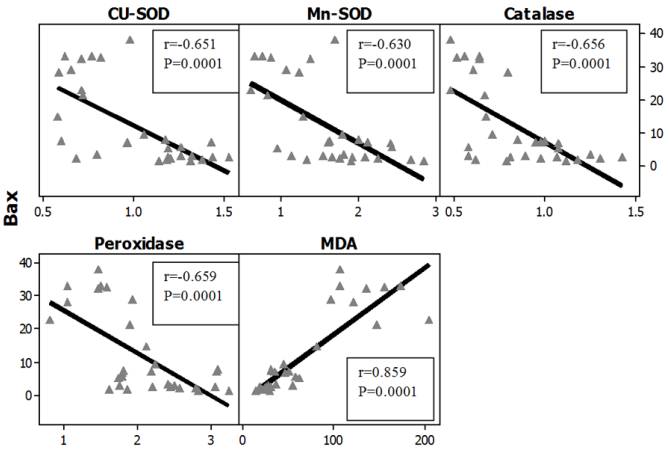

Figure 27. Correlations between apoptotic index (Bax) with antioxidant enzymes gene expression in all studied groups in the Brain. r: Pearson Correlation coefficient; P: Probability.

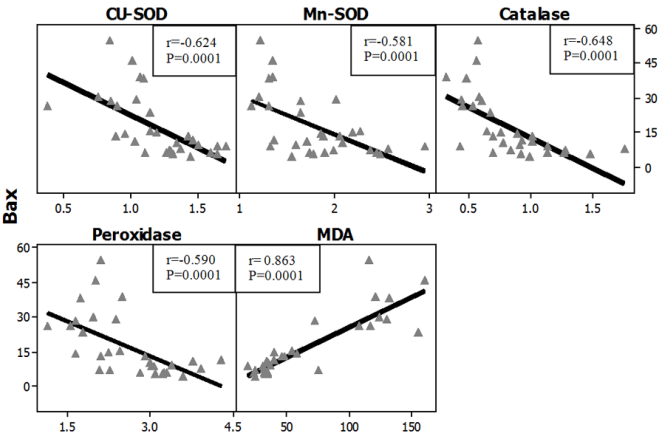

Figure 28. Correlations between apoptotic index (Bax) with antioxidant enzymes gene expression in all studied groups in the testes. r: Pearson Correlation coefficient; P: Probability.

electron transfer process to this complex from reduced ubiquinone. The brain is particularly susceptible to oxidative damage due to its high levels of oxygen consumption, increased levels of polyunsaturated fatty acid and relatively low levels of antioxidants [29]. Chronic administration of tramadol to mice resulted in oxidative stress in brain tissues. This effect was associated with a significant decrease in brain non-enzymatic antioxidant, intracellular reduced glutathione level and in enzymatic antioxidant, glutathione peroxidase activity [30]. Moreover, it has been reported that oxidative modifications result in a loss of function and lowering of enzyme activity [31]. Another explanation was presented by [32] as they demonstrated a long-term effect of tramadol on neuronal glucose metabolism and insulin signaling pathway in the cerebral cortex which consequently leads also to development of oxidative stress.

Oxidative stress induced by tramadol on different organs by induction of inflammatory reaction that is effectively reduced after withdrawal period was explained by [21]. This inflammatory reaction proved previously to be a causative factor for oxidative stress by inducing changes in cell membrane fatty acid composition in rabbits following tramadol administration leading to a decrease of its fluidity, which in turn will impair formation of pseudopodia and internalization of pathogens and foreign particles [33].

Recently, [34] found a similar finding in testicular tissue as they reported that tramadol increased the testicular levels of nitric oxide and lipid peroxidation and decreased the anti-oxidant enzymes activities significantly compared with the control group as well as immunohistochemical examinations showed that tramadol increased the expression of endothelial nitric oxide synthase in testicular tissues. They concluded that tramadol treatment affects the testicular function of adult male rats, and these effects might be through the overproduction of nitric oxide and oxidative stress induced by this drug.

The current study showed that Bax- immunohistochemically positive cells which is indicated as apoptotic index increased in group II than in group I while it decreased in group III than group II and non-significant increase in group III when compared to group I was observed. This indicates that there is an increase in apoptosis in both cerebral cortex and testicles in rats receiving tramadol which subsides when the drug become withdrawn.

These findings coincide with that reported by [2]. They stated that the multiple effects of opioids on neuronal structure (cytoskeleton) have been regarded as the markers of neuronal damage due to long term use of morphine and

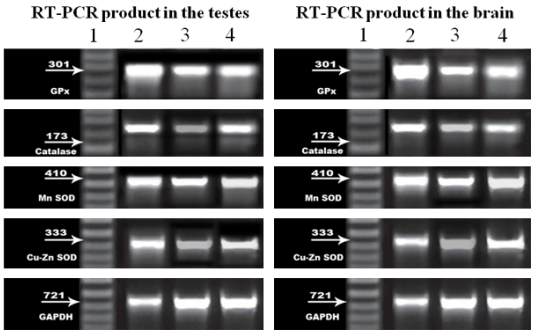

Figure 29. Semiquantitative RT-PCR of genes of antioxidant enzymes of testicular and brain tissues. RT-PCR product of antioxidant enzymes and GAPDH expression in rats of all of the studied groups: Lane1: The DNA marker, Lane 2: RT-PCR products in control group (I) Lane 3: RT-PCR products in group (II), Lane 4: RT-PCR product in group (III).

other opioids. It may also induce the mRNA expression of pro-apoptotic receptors in the lymphocytes and mouse spleen, lung and heart via activating opioid receptor. They observed large amount of apoptotic neurons in the hippocampus of these rats, and the expressions of the apoptosis related proteins (Fas, Bcl-2 and caspase-3) presented with alteration. When compared with control group, the expressions of Fas and caspase-3 increased markedly and Bcl-2 expression reduced significantly in morphine addiction group and morphine abstinence group. These suggest that long term use of morphine as example of opoid drug may increase the apoptotic neurons via apoptosis related signaling pathway. This also confirmed by a result presented previously by [35] as they concluded that chronic use of morphine and/or tramadol in increasing doses is found to cause red neuron degeneration and apoptosis in the rat brain, which probably contributes to cerebral dysfunction.

Recently, [6, 7] demonstrated that chronic treatment of rats with opiate is associated with a remarkable upregulation of the pro-apoptotic Fas receptor, as well as intracellular pro-apoptotic elements such as caspase-3, combined with an opposing moderate down-regulation of the anti-apoptotic oncoprotein Bcl-2.

In our study, the apoptotic index was increased in testicular tissue of rats under tramadol administration than the control group and decreased in rats under withdrawal. These results coincide with a similar study dealing with Methadone and Buprenorphine opioids (similar in action to tramadol) by [36]. They presented histological picture of apoptosis in rats receiving these drugs and they reported that methadone and buprenorphine are opioids that have effects on spermatogenesis and secondary sex organs.

By light microscopic examination of the testicles of tramadol treated rats, the results of the current study demonstrated that the seminiferous tubules appeared with irregular outline and widely separated from each other with absence of spermatozoa. Many vacuoles among the spermatogenic cells, apoptotic cells and multinucleated giant cells were found. The intertubular tissue was degenerated and showed many inflammatory cells and leydig cells were reduced in number. The majority of the seminiferous tubules exhibited damaged and disorganized spermatogenetic cells and the damaged germ cells were lifting off the basal lamina and some of them were exfoliated in the lumen. The reduction of Sertoli and Leydig cells by opiates was also observed by [37]. They explained this by disorders in the endocrine and paracrine function that can indirectly influence the final size of sertoli cell population through disordered LH, estradiol, somatotropin, somatostatin, prolactin and GnRH (gonadotropin-releasing hormone) acted upon either on the hypothalamus or directly on pitutary glands. In addition to opiate induced reduction of serum testosterone level there is abnormal structural and functional abnormalities of the secondary sex organs, it seems probable that opiates could affect testes volume and induce arrested spermatogenesis, sloughed germinal epithelium, destroyed sertoli cells and thickened and irregular basement membrane as well as signs of apoptosis [36].

The giant multinucleated cells might result from widening of the intercellular bridge between adjacent spermatids resulting in subsequent fusion of two or more cells [38]. Also, another study revealed that the testes undergo severe diffused testicular degeneration with numerous spermatocyte and spermatid giant cell formation (the cells might be fused together to form such giant cells) without spermatogenesis after tramadol in a dose of 40 mg/kg b.wt. The spermatocytes were mostly necrotic [39].

This result also confirmed by another study that postulated that testicular cells and sperm are susceptible to oxidative damage by free radicals as their plasma membrane contains abundance of polyunsaturated fatty acid [40]. Lipid peroxidation of the cellular membrane may eventually result in dysfunction and structural damage of the cell [41]. Therefore, the abnormalities observed in the testicular structures including germ and Leydig cells found in this study might be attributed to the peroxidation of polyunsaturated fatty acids in their plasma membranes by tramadol.

By transmission electron microscope of tramadol treated group, the seminiferous tubules appeared with a wavy thickened basement membrane and the interstitial tissue showed eosinophils and congested capillaries. The same findings were described previously by [36]. Moreover, thickening of the basement membrane of seminiferous tubules, reduction of tubular diameter and germinal epithelium height, cell-maturation arrest were also observed previously by [42]. These findings also are in agreement and explained by [43] as they postulated that changes in the thickness of the basement membrane can impair testicular metabolism, and thus promotes enhanced germinal cell hypoplasia and tubular atrophy. The extent of testicular damage is closely related to the duration of drug consumption.

In our study, there were histological changes in the form of degeneration of the nuclei of spermatogonia, many disrupted mitochondria in the cytoplasm and numerous vacuoles in-between the cells. The primary spermatocytes appeared with disrupted and less peripheral mitochondria and its nucleus showed clumps of a peripheral dense chromatin.

The observed mitochondrial changes might be considered as early manifestation of apoptosis and an adaptative process to unfavorable environments as excess exposure of the cell to free radicals at the level of intracellular organelles. These suggestions might be confirmed by the successful suppression of these changes by free radical scavengers [44].

In group III (rats under tramadol withdrawal), most of the seminiferous tubules appeared with increased spermatogenic cell layers and with increase in the number of sperm bundles. The spaces between the seminiferous tubules were reduced in size. Electron microscopic examination of testes of rats of this group showed the seminiferous tubules with intact basal lamina and intact spermatogonic cells regardless some spermatid appeared with shrunken nucleus.

As regard cerebral cortex, apoptosis was proved in cerebral cortex of tramadol treated rats by light microscopic examination as there was marked cortical layers disorganization and hypercellularity as well as increased apoptotic cells. Additionally, extensive neuropil vacuolization and multinuclear giant cells were also seen. Degenerated pyramidal cells appeared either darkly stained with pyknotic nuclei or with faintly stained cytoplasm and nuclei. Some pyramidal cells were shrunken and showed marked cytoplasmic vacuolization. This vacuolation could be attributed to the damaged cell organoid from exposure to free radicals [10, 45]. Some regions of the neuropil showed dilated blood vessels, cellular infiltrate and red neurons (neurons with hypoxic changes) which coincides with the results that observed by [28]. They listed their histological finding of brain and revealed that pyramidal cells lost its shape, perivascular space increased with hemorrhage, disrupted ependyma, and choroid plexus became hypertrophied. These results were also observed by another study done by [39] as they found congestion of submeningeal blood vessels and neural degeneration following tramadol. Moreover, [2] found that the apoptotic cells were present with cytoplasmic contraction, reduction in cell volume and nuclear condensation. The apoptotic cells were detached from surrounding cells by Tunnel technique in addition to large amount of apoptotic signals were observed in the nucleus of neurons in the group utilizing opiate as they utilized morphine in their study.

In group III, most of the histological findings were subsided as there was return of brain tissues towards normal morphology as evidenced by decreased cellularity and decreased perineuronal haloes as well as normal blood vessels. Multiple pyramidal cells and granular cells appeared normal; however, few pyramidal cells are shrunken and surrounded by haloes. This indicates that the apoptosis activity as well as the oxidative stress damage of brain tissue mostly decreased in this group. These results are in agreement with [46]. They stated that whereas rats examined after the withdrawal

recovery period unlikely showed complete recovery (did not return back to normal control) but marked reduction in cellular damage was observed when compared to tramadol treated groups.

In conclusion, based on the above results and discussion, it could be concluded that administration of tramadol have histological abnormalities on both cerebral cortex and testicular tissues associated with oxidative stress in these organs due to elevation of lipid peroxidation products with inhibition of antioxidant enzymes gene expression leading to imbalance between oxidant/antioxidant ratio. Also, there is increase in apoptosis in both organs which demonstrated by increase in Bax-immounohistochemical positive cells denoted by apoptotic index. Light microscopic examination of both organs as well as electron microscopic examination of testicular tissue comes to prove the toxic effects of tramadol and this means that it exerts its toxic effect through 2 possible synerergestic mechanisms of action, oxidative stress as well as apoptosis. Tramadol withdrawal has better histological and biochemical picture than those under usage in-spite of that it is not returned back to normal but it is associated with good future for tramadol users. Finally, these findings may provide a possible explanation for the unexplained delayed fertility as well as behavioral and psychological changes associated with tramadol abuse.

Tramadol abuse should be avoided without medical description due to its toxic effects. Users of tramadol under withdrawal should consult neurologist and andrologist to minimize its residual undesirable effects. Further investigations are needed for more comparison and interpretation.

Disclosure of conflict of interest

None.

Address correspondence to: Dr. Ayman Z Elsamanoudy, Department of Medical Biochemistry and Molecular Biology, Faculty of Medicine, Mansoura University, Egypt. E-mail: ayman.elsamanoudy@gmail.com

References

[1] Liu H, Liu Z. The investigation of tramadol dependence with no history of substance abuse: a cross-sectional survey of spontaneously reported cases in Guangzhou City, China. Biomed Res Int 2013; 2013: 283425.

[2] Liu LW, Lu J, Wang XH, Fu SK, Li Q, Lin FQ. Neuronal apoptosis in morphine addiction and its molecular mechanism. Int J Clin Exp Med 2013; 6: 540-5.

[3] Ghosian Moghaddam MH, Khalili M, Maleki M, Ahmad Abadi ME. The Effect of Oral Feeding of Tribulus terrestris L. on Sex Hormone and Gonadotropin Levels in Addicted Male Rats. Int J Fertil Steril 2013; 7: 57-62.

[4] Bodera P, Stankiewicz W, Zawada K, Antkowiak B, Paluch M, Kieliszek J, Kalicki B, Bartosiński A, Wawer I. Changes in antioxidant capacity of blood due to mutual action of electromagnetic field (1800 MHz) and opioid drug (tramadol) in animal model of persistent inflammatory state. Pharmacol Rep 2013; 65: 421-8.

[5] Bajic D, Berde CB, Commons KG. Periaqueductal gray neuroplasticity following chronic morphine varies with age: role of oxidative stress. Neuroscience 2012; 226: 165-77.

[6] Sharifipour M, Izadpanah E, Nikkhoo B, Zare S, Abdolmaleki A, Hassanzadeh K, Moradi F, Hassanzadeh K. A new pharmacological role for donepezil: attenuation of morphine-induced tolerance and apoptosis in rat central nervous system. J Biomed Sci 2014; 23: 21-6.

[7] Hassanzadeh K, Habibi-Asl B, Farajnia S, Roshangar L. Minocycline prevents morphine-induced apoptosis in rat cerebral cortex and lumbar spinal cord: a possible mechanism for attenuating morphine tolerance. Neurotox Res 2011; 21: 649-659.

[8] Matthiesen T, Wöhrmann T, Coogan TP, Uragg H. The experimental toxicology of tramadol: an overview. Toxicol Lett 1998; 95: 63-71.

[9] Bancroft JD, Gamble M. Theory and Practice of Histological Technique. 5th edition. Edinburg and London: Churchill Livingstone; 2002.

[10] Zarnescu O, Brehar FM, Chivu M, Ciurea AV. Immunohistochemical localization of caspase-3, caspase-9 and Bax in U87 glioblastoma xenografts. J Mol Histol 2008; 39: 561-569.

[11] Xu C, Shu WQ, Qiu ZQ, Chen JA, Zhao Q, Cao J. Protective effects of green tea polyphenols against subacute hepatotoxicity induced by microcystin-LR in mice. Environ Toxicol Pharmacol 2007; 24: 140-148.

[12] Bozzola JJ, Russell LD. Electron microscopy: Principles and techniques for biologists. 2nd edition. Jones & Bartlett Publishers; 1998.

[13] Raha S, Ling M, Merante F. Extraction of total RNA from tissues and cultured cells. In: Molecular Biomethods Handbook. Replay R, Walker JM, editors. Totowa, NJ: Human Press Inc; 1998. pp. 1-8.

[14] Berchtold MW. A simple method for direct cloning and sequencing cDNA by the use of a single specific oligonucleotide and oligo (dT) in a polymerase chain reaction (PCR). Nucleic Acids Res 1989; 17: 453.
[15] Laybutt DR, Kaneto H, Hasenkamp W, Grey S, Jonas JC, Sgroi DC, Groff A, Ferran C, Bonner-Weir S, Sharma A, Weir GC. Increased expression of antioxidant and antiapoptotic genes in islets that may contribute to beta-cell survival during chronic hyperglycemia. Diabetes 2002; 51: 413-23.
[16] Rozen S, Skaletsky HJ. (1998) Primer3 (v. 0.9) (Whitehead Institute for Biomedical Research). Code available at http://www genome.wi.mit.edu/genome_software/other/primer3.html. Last access: 2004.
[17] Buege JA, Aust SD. Microsomal lipid peroxidation. Methods Enzymol 1972; 52: 302-10.
[18] Dawson B, Trapp R. Basic and clinical biostatistics: large medical books. Oxford, London, Boston; 2001. pp. 270-275.
[19] El-Gaafarawi II. Biochemical toxicity induced by tramadol administration in male rats. Egyptian Journal of Hospital Medicine 2006; 23: 353-362.
[20] Popovic M, Janicijevic-Hudomal S, Kaurinovic B, Rasic J, Trivic S, Vojnović M. Antioxidant effects of some drugs on immobilization stress combined with cold restraint stress. Molecules 2009; 14: 4505-16.
[21] Rabei HM. The immunological and histopathological changes of Tramadol, Tramadol/Acetaminophen and Acetaminophen in male Albino rats "Comparative study". The Egyptian Journal of Hospital Medicine 2011; 45: 477-503.
[22] Costa PF, Nunes N, Belmonte EA, Moro JV, Lopes PCF. Hematologic changes in propofol-anesthetized dogs with or without tramadol administration. Arq Bras Med Vet Zootec 2013; 65: 1306-1312.
[23] McKeon GP, Pacharinsak C, Long CT, Howaed AM, Jampachaisri K, Yeomans DC, Felt SA. Analgesic effects of tramadol, tramadol - gabapentin, and buprenorphine in an incisional model of pain in rats (Rattus norvegicus). J Biol Chem 2011; 286: 16186-96.
[24] Panchenko LF, Pirozhkov SV, Nadezhdin AV, Baronets VI, Usmanova NN. Lipid Peroxidation, Peroxyl Radicalscavenging System of Plasma and Liver and Heart Pathology in Adolescence Heroin Users. Vopr Med Khim 1999; 45: 501-506.
[25] Zhang YT, Zheng QS, Pan J, Zheng RL. Oxidative Damage of Biomolecules in Mouse Liver Induced by Morphine and Protected by Antioxidants. Basic Clin Pharmacol Toxicol 2004; 95: 53-58.
[26] Atici S, Cinel I, Cinel L, Doruk N, Eskandari G, Oral U. Liver and Kidney Toxicity in Chronic Use of Opioids: An Experimental Long Term Treatment Model. J Biosci 2005; 30: 245-252.
[27] Lemarie A, Grimm S. Mutations in the heme b-binding residue of SDHC inhibit assembly of respiratory chain complex II in mammalian cells. Mitochondrion 2009; 9: 254-260.
[28] Mohamed TM, Abdel Ghaffar HM, El Husseiny RM. Effects of tramadol, clonazepam, and their combination on brain mitochondrial complexes. Toxicol Ind Health 2013; [Epub ahead of print].
[29] Butterfield DA, Castegna A, Lauderback CM, Drake J. Evidence that amyloid beta-peptide-induced lipid peroxidation and its sequelae in Alzheimer's disease brain contribute to neuronal death. Neurobiol Aging 2002; 23: 655-64.
[30] Abdel-Zaher AO, Abdel-Rahman MS, ELwasei FM. Protective effect of Nigella sativa oil against tramadol-induced tolerance and dependence in mice: Role of nitric oxide and oxidative stress. NeuroToxicology 2011; 32: 725-733.
[31] Butterfield DA, Reed T, Newman SF, Sultana R. Roles of amyloid beta-peptide-associated oxidative stress and brain protein modifications in the pathogenesis of Alzheimer's disease and mild cognitive impairment. Free Radic Biol Med 2007; 43: 658-77.
[32] Kanter M. Nigella sativa and derived thymoquinone prevent hippocampal neurodegeneration after chronic toluene exposure in rats. Neurochem Res 2008; 33: 579-88.
[33] Alici HA, Ozmen I, Cezur M, Sahin F. Effect of the spinal drug tramadol on the fatty acid compositions of rabbit spinal cord and brain. Biol Pharm Bull 2003; 26: 1403-6.
[34] Ahmed MA, Kurkar A. Effects of opioid (tramadol) treatment on testicular functions in adult male rats: The role of nitric oxide and oxidative stress. Clin Exp Pharmacol Physiol 2014; 41: 317-23.
[35] Atici S, Cinel L, Cinel I, Doruk N, Aktekin M, Akca A, Camdeviren H, Oral U. Opioid neurotoxicity: comparison of morphine and tramadol in an experimental rat model. Int J Neurosci 2004; 114: 1001-11.
[36] Heidari Z, Mahmoudzadeh-Sagheb H, Kohan F. A Quantitative and Qualitative Study of Rat Testis Following Administration of Methadone and Buprenorphine. International Journal of High Risk Behaviors and Addiction 2012; 1: 14-17.
[37] Caju FM, Gian, Queiroz GCD, Torres SM, Tenório BM, Júnior VMS. Opioid system manipulation during testicular development: results on sperm production and sertoli cells population. Acta Scientiarum Biological Sciences 2011; 33: 219-225.
[38] Hess RA, Nakai M. Histopathology of the male reproductive system induced by the fungicide

benomyl. Histol Histopathol 2000; 15: 207-224.
[39] Abou El Fatoh MF, Farag M, Sayed AE, Kamel MA, Abdel-Hamid N, Hussein M, Salem GA. Some Biochemical, Neurochemical, Pharmacotoxicological and Histopathological Alterations Induced by Long-term Administration of Tramadol in Male Rats. Int J Pharm Sci 2014; 4: 565-571
[40] Alvarez JG, Storey BT. Differential incorporation of fatty acids into and peroxidative loss of fatty acids from phospholipids of human spermatozoa. Mol Reprod Dev 1995; 42: 334-346.
[41] Smith C, Marks AD, Liebermann ML. Mark's Basic Medical Biochemistry: A Clinical Approach. Oxygen Toxicity and Free Radical Injury. 2nd edition. Baltimore MD, editor. USA: Lippincott Williams & Wilkins; 2005. pp. 439-457.
[42] Reuhl J, Bachl M, Schneider M, Lutz F, Bratzke H. Morphometric assessment of testicular changes in drug-related fatalities. J Forensic Sci Int 2001; 115: 171-81.
[43] Sorge RE, Stewart J. The effects of long-term chronic buprenorphine treatment on the locomotor and nucleus accumbens dopamine response to acute heroin and cocaine in rats. J Pharmacol Biochem Behav 2006; 84: 300-5.
[44] Wakabayashi T. Megamitochondria formation-physiology and pathology. J Cell Mol Med 2002; 6: 497-538.
[45] Brown DM, Donaldson K, Borm PJ, Schins RP, Dehnhardt M, Gilmour P, Jimenez LA, Stone V. Calcium and ROS-mediated activation of transcription factors and TNFalpha cytokine gene expression in macrophages exposed to ultrafine particles. Am J Physiol Lung Cell Mol Physiol 2004; 286: L344-L353.
[46] Khodeary MF, Sharaf El-Din AI, El Kholy SMS. A histopathological and immunohistochemical study of adult rats'brain after long term exposure to amadol (tramadol hydrochloride). Mansoura J Forensic Med Clin Toxicol 2010; 18: 1-24.